SIMULATE-3K PEACH BOTTOM 2 TURBINE TRIP 2 BENCHMARK CALCULATIONS

Lotfi A. Belblidia and Gerardo M. Grandi
Studsvik Scandpower Inc.
702 Russell Ave, Suite 405, Gaithersburg, MD 20877
lotfi@soa.com; gerardo@soa.com

Christian Jönsson
Studsvik Scandpower AB
Hantverkargatan 2A, S2722 12 Västerås, Sweden
Christian.Jonsson@studsvik.se

ABSTRACT

This paper discusses the model and results for the Peach Bottom 2 Turbine Trip Test 2 using Studsvik Scandpower's transient code SIMULATE-3K. This transient is currently the subject of a NEA/OCED BWR benchmark. All data pertaining to core, vessel, and scenario were taken from the benchmark specifications. The nuclear data were generated with Studsvik Scandpower lattice's code CASMO-4 and core analysis code SIMULATE-3. Comparisons to measured data, sensitivity to model options and data, as well as results from a more limiting scenario are presented. SIMULATE-3K captures well the parameters of importance in this transient, namely the pressure wave propagation, the void collapse during the pressurization phase and the resulting power peak.

1. INTRODUCTION

The Nuclear Energy Agency (NEA) of the Organization for Economic Cooperation and Development (OECD) has proposed as a benchmark for a BWR plant transient the Peach Bottom Turbine Trip Test 2 (TT2) [1]. This pressurization transient, in which the coupling between the core and system dynamics plays an important role, includes real plant data making it very valuable for validating best-estimate analysis codes. For this purpose, a SIMULATE-3K [2-5] model for this plant was set up using the data provided in the specifications.

Several aspects govern this transient: the velocity of the pressure wave from the turbine stop valve to the core, the void collapse rate which produces the power excursion, the void production caused by the power spike which turns the power around and produces the pressure increase in the system. Ultimately, the power excursion is halted by the insertion of the control rods. The behavior of the initial phase of the transient is controlled by the rate on closure of the turbine stop valve and the opening of the turbine bypass valve, both of which are specified as boundary conditions in this benchmark.

A brief overview of the methods in SIMULATE-3K is provided next. The work is described in Section 3. Section 4 gives the best-estimate SIMULATE-3K results together with comparisons to measured data.

2. DESCRIPTION OF SIMULATE-3K

2.1 NEUTRONICS

SIMULATE-3K (S3K) solves the 3D, two-energy group neutron diffusion equation with one radial node representing each fuel assembly and typically 25 axial nodes for the active height, and explicit radial and axial reflectors. The S3K model uses a fourth-order flux expansion [6] for the neutron flux distribution within each node in each of the three directions and the spatial gradient of the flux is represented by a third-order function rather than the traditional first-order methods. Furthermore, assembly discontinuity factors [7] are used to model heterogeneities in the presence of burnable absorbers.

The frequency transform method is used to solve the transient diffusion equations by separating the flux into a pure exponential time dependent component and a primarily spatial and weakly temporal dependent component. The Cyclic Chebyshev Semi-Iterative method is used for the flux iterations at each time step to solve for new flux values, and an optimum over-relaxation factor is calculated to maximize the convergence rate.

The code tracks dynamically nodal concentration of fission products and accounts for the extraneous neutron sources due to spontaneous fissions, alpha-n interactions from actinide decay, and gamma-n interactions from long-term fission product decay. This is of most importance for subcritical start-up simulations. Decay heat is modeled by using the ANSI/ANS-5.1 23-group data for U-235, U-238, and Pu-239 fissions [8]

SIMULATE-3K performs a pin-by-pin power reconstruction over the whole core and computes LPRM, IRM, and SRM signals

2.2 PIN CONDUCTION MODEL

Fuel pin temperatures and heat fluxes are computed using a fully implicit time dependent one-dimensional radial heat conduction equations. The fuel properties depend on burnup and temperature, and the heat fluxes are solved at each time step by nonlinear iteration.

SIMULATE-3K uses fuel and clad properties from MATPRO. The gap conductance is calculated as a function of burnup and temperature. The model embedded in S3K is similar to those of the Studsvik Scandpower's fuel performance code INTERPIN [9].

2.3 CHANNEL HYDRAULICS

The core is represented with one thermal-hydraulic channel per fuel bundle with no cross flow and variable axial meshing. The hydraulic model uses optionally five or six equations. It is fully implicit linear nodal model and accounts for unknowns at the edges of the control cell (i.e., no mesh staggering). No linearization is introduced and at each time step there is a complete solution of the nonlinear equations.

2.4 VESSEL HYDRAULICS

The vessel is composed of upper plenum, standpipes, steam separators, downcomer (with 2 radial non-mixing zones), two recirculation loops, lower plenum (with 2 radial non-mixing zones), and steam dome [5]. It also includes one recirculation pump in each recirculation loop and a model for the

jet pumps. The vessel model is based on a five-equation model, similar to the core channel hydraulics. It is intended for use in non-LOCA transients.

Homologous pump curves provide the pressure rise in the recirculation pumps as a function of flow rate and pump speed. The jet pump model consists of a mixing section in which the drive flow from a recirculation loop is mixed with the suction flow. It provides the pressure increase at the jet pump location as a momentum jump condition and neglects inertia and gravity effects. The steam separator model includes flow inertia in the separators, pressure losses, and carry-under flow.

2.5 STEAM LINE MODEL

The S3K steam-line model was taken from RAMONA [10]. It is capable of simulating acoustic effects in the steam line due to sudden valve closures and openings. The model consists of a single pipe (with areas that can change at branch locations) connecting the steam dome to the turbine stop valve. Two branches are modeled: one at the SRV location and the other leading to the turbine bypass valve. Main steam isolation valves are also modeled as well as a pressure controller.

3. DESCRIPTION OF WORK

A SIMULATE-3 model for Peach Bottom was set up and depleted for two cycles until the end of cycle 2 corresponding to the point at which the turbine trip transients were conducted. SIMULATE-3 is Studsvik Scandpower's core analysis code. The restart file from these calculations together with the CASMO-4 library file for the lattices in the Cycle 2 core loading were used in SIMULATE-3K. All data pertaining to the core (loading, assembly dimensions, pin enrichments, loss coefficients, etc.) were taken from the specifications, except for the fuel properties which were based on the internal S3K models .

The RETRAN deck provided with the specifications was used to construct a model for the vessel (downcomer, upper and lower plena, steam standpipes and separators, steam dome), jet pumps, recirculation pumps, and steam line. The separator loss coefficient was adjusted to produce the pressure drop between upper plenum and steam dome given by the vendor equation and provided with the specifications. Similarly jet pump data (areas and loss coefficients) were tuned to generate the correct drive flow and M and N ratios.

The following boundary conditions were applied in the base calculations:

- Flow versus time at the turbine stop valve position
- Turbine bypass valve position versus time
- Measured feedwater flow versus time
- Constant feedwater temperature
- Delayed scram activation past the power peak (to ensure no impact of the scram on the power peak)

The calculation of TT2 was followed by more limiting cases:

- No scram
- No bypass valve opening and scram signal initiated at 95% power
- No bypass valve opening and no scram

A number of sensitivity calculations to model options and data were also performed.

4. RESULTS

Table 1 shows the steady-state initial conditions prior to the transient and comparison with measured data. Figure 1 shows the initial distributions for the average axial power and the comparison to the data from the P1 edit.

Transient results for the base turbine trip case are illustrated in Figures 2 through 5. The transient power behavior is compared to the measured average LPRM signal in Figure 2. The peak relative power is well predicted at 4.43 (measured value 4.52). The time of the peak is delayed by about 0.06 sec (0.78 sec versus 0.72 sec from start of turbine stop valve closure).

Steam dome pressure is compared to measured data in Figure 3. A time shift of 50 msec was applied to the measured steam dome pressure to account for the test acquisition time delays. Calculated steam dome pressure and core upper plenum pressure are shown for the initial part of the transient in Figure 4. This figure clearly shows the pressure wave propagation between steam dome and core exit and the delay of about 50 msec associated with it.

The calculated water level behavior captures well the overall trend shown in the measurement. There are some differences during the initial phase of the transient and a bias of about 0.17 m. A comparison plot is given in Figure 5.

The calculations capture very well the overall trend of the pressure behavior. Some differences between calculations and measurements appear beyond the peak after about 3 seconds in the transient. The calculated pressure decrease at a faster rate. This could be due to the modeling of the stored energy in the fuel, the rate at which it is released to the coolant, or the rate of steam production after the scram. Other factors that may play a role are overestimation of the bypass valve capacity and of the amount of subcooled water that enters the core.

Several model parameters influence the results, both the peak power reached and the timing of the peak. Among these, the most sensitive are the void coefficient, the gap conductance, and the steam separator inertia. The void coefficient is determined by the cross section density dependence and is fixed by the lattice code and the nuclear data library used in the cross section generation. The gap conductance depends on fuel type, dimensions, exposure and temperature. There is large uncertainty attached to the steam separator inertia to account for the swirling of the mixture as it travels through the steam separator barrels. An effective L/A based on a GE model was used in the base TT2 calculations, with a typical value for the curve intercept at zero quality.

Figure 6 shows the sensitivity of the power peak to the steam separators inertia. Three different calculations are compared: (a) reference with typical value for L/A at zero void, (b) effective L/A model is removed (i.e. the geometrical L/A ratio is used), and (c) the value of L/A at zero void was increased by 20%. If the steam separator inertia model is not activated (geometrical L/A) then the power peak is reduced and further delayed. If the inertia is increased then the relative power peak (4.54 instead of 4.33) is closer to the measured value. The timing of the peak is slightly reduced (from 0.78 sec to 0.77 sec).

Figure 7 shows the effect of the gap conductance. Two cases are compared: (a) the reference solution using the default gap conductance values and (b) the solution obtained with the gap conductance is based on the data provided in the benchmark specifications. The later case predicts lower gap

conductances and therefore a higher relative power peak (5.17 instead of 4.33). The timing of the peak is slightly more delayed compared to the base case (0.08 sec instead of 0.06 sec).

Figure 8 shows the effect of the void coefficient. Two cases are compared: (a) the reference solution, and (b) the solution applying a void coefficient multiplier of 1.2. The increase of the density feedback significantly increases the peak power and reduces its time delay.

In order to investigate the effect of the bypass valve capacity on the depressurization rate after the scram, the bypass valves capacity was reduced 20%. Figure 9 and 10 illustrate the effect of the bypass flow. The case with lower bypass valve capacity reaches higher pressures and consequently results in a higher power peak power. The timing of the peak power is not changed. Note that the reduction of the bypass valve capacity does not significantly change the depressurization rate after 3 sec.

The more severe transients are illustrated by Figures 11 and 12. These figures show the responses of power, dome pressure and SRV flow for the case with no scram and no opening of the turbine bypass valve. The power shows several peaks caused by the pressurization and limited by the Doppler and void feedback. Cycling of the relief valves occurs during this transient causing the dome pressure to remain within a range of the SRV opening and closing setpoints. The closure setpoints were taken to be 97% of the opening setpoints and no time delays were used for the valve closings.

CONCLUSIONS

A SIMULATE-3K model for the Peach Bottom Turbine Trip Test 2 was successfully implemented and exercised. The code captures well the parameters of importance in this transient, namely the pressure wave propagation, the void collapse during the pressurization phase, and the void and Doppler reactivity feedbacks. Some differences with the measurements were observed with respect to the timing of the power peak during TT2 and the rate of depressurization following the scram. Evaluation of the model and code improvement is an ongoing effort.

ACKNOWLEDGEMENTS

This work benefited from the significant help of Lars Moberg, Jeffrey Borkowski and Kord Smith of Studsvik Scandpower. Our special thanks go to Sven-Birger Johannesson who set up the SIMULATE-3 model and performed the core follow calculations in our Västerås office.

REFERENCES

1. Jorge Solis *et al.*, "Boiling Water Reactor Turbine Trip (TT) Benchmark, Volume I: Final Specifications," Rev. 1, NEA/NSC/DOC(2001)1, Rev 1, October 2001.
2. J. Borkowski *et al.*, "A Three-Dimensional Transient Analysis Capability for SIMULATE-3," *Trans. Am. Nucl. Soc.*, **71**, 456 (1994).
3. J. Borkowski *et al.*, "SIMULATE-3K Simulations of the Ringhals-1 BWR Stability Measurements," *Proceedings PHYSOR 1996*, Mito, Ibaraki, Japan, September 16-20, 1996.
4. J. Borkowski *et al.*, "Best-Estimate Three-Dimensional Transient Analysis Using Design-Basis Methodology," *Int. Meeting on "Best-Estimate" Methods in Nuclear Installations Safety Analysis (BE-2000)*, Washington, D.C., November, 2001.

5. Gerardo M. Grandi and Kord S. Smith, "BWR Stability Analysis with SIMULATE-3K," *Proc. PHYSOR 2002*, Seoul, Korea, October 7-10, 2002.
6. K.S. Smith, "QPANDA: An Advanced Nodal Method for LWR Analysis," *Trans. Am. Nucl. Soc.*, **50**, 532 (1985).
7. K.S. Smith, "An Assembly Homogenization Techniques for Light Water Reactor Analysis," *Prog. Nucl. Energy*, **17**, 303 (1986).
8. "American National Standard for Decay Heat Power in Light Water Reactors," ANS/ANSI-5.1-1994, American Nuclear Society (1994).
9. J.T. Cronin, K.S. Smith, and J.A. Umbarger, "INTERPIN-CS User's Manual," Studsvik Scandpower (1995).
10. G.M. Grandi, "RAMONA-5 User Manual," Studsvik Scandpower (2001).
11. N.H. Larsen, "Core Design and Operating Data for Cycles 1 and 2 of Peach Bottom 2," NP-563, Electric Power Research Institute (1978).

Table 1: Initial conditions

Parameter	S3K Value	Specifications Value
Relative power (%)	61.60	61.65
Relative flow (%)	80.9	-
Thermal power (MWT)	2030	2030
Total core flow (kg/s)	10445	10445
Bypass flow (kg/s)	781.4	841.68
Bypass flow fraction (%)	7.48 (♣)	8.06
Inlet subcooling (kJ/kg)	48.3	48.0
Inlet enthalpy (kJ/kg)	1208.7	-
Inlet temperature (^{o}C)	274.6	-
Dome pressure (MPa)	6.7989	6.7985
Core exit pressure (MPa)	6.8640	-
Core pressure drop (MPa)	0.104430	0.083567
Standpipes and separator loss	0.054736	0.049828
Core average exit quality (%)	9.42	9.52
Average void (%)	30.4	30.4
k-effective	0.99150	-
Feedwater flow (kg/s)	980.8	980.3
Recirculation flow (kg/s)	5222.0	5222.5
Jet pump drive flow (kg/s)	2964.7	2871.2
Jet pump M factor	2.523	2.638
Jet pump N factor	0.17	0.17

(♣) Bypass flow based on Figure 55 of EPRI Report NP-563 [11]. Specifications value does not match the design data in this report

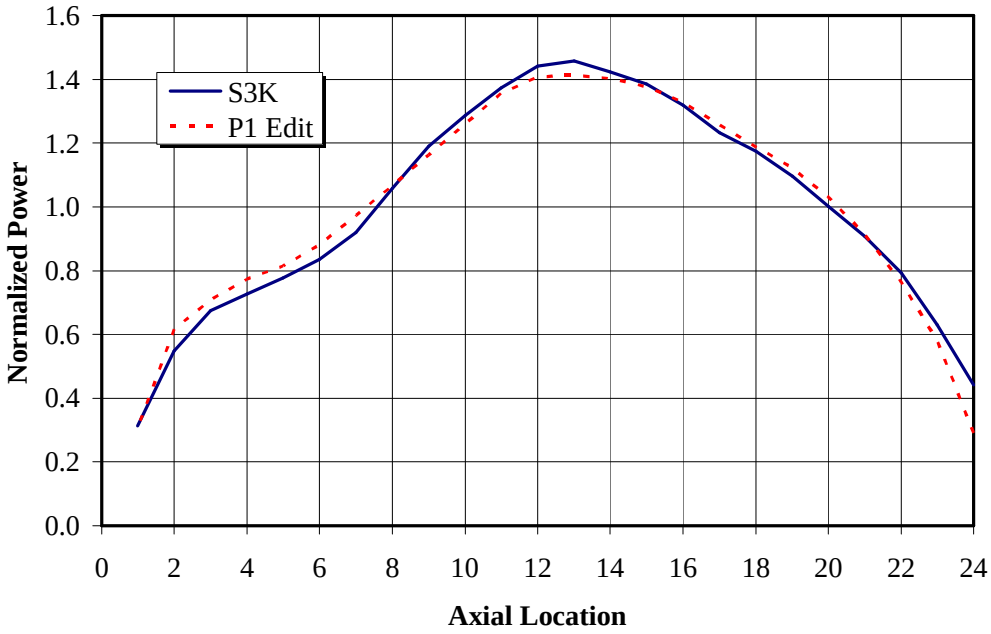

Figure 1. Initial average axial power distribution.

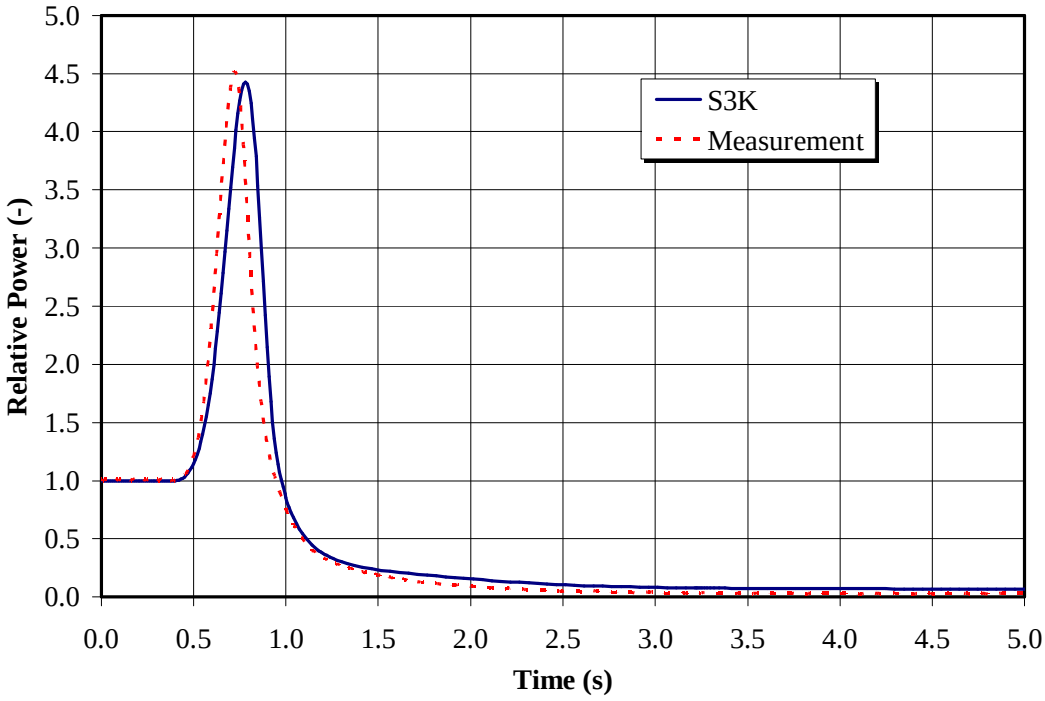

Figure 2. Relative power behavior during TT2.

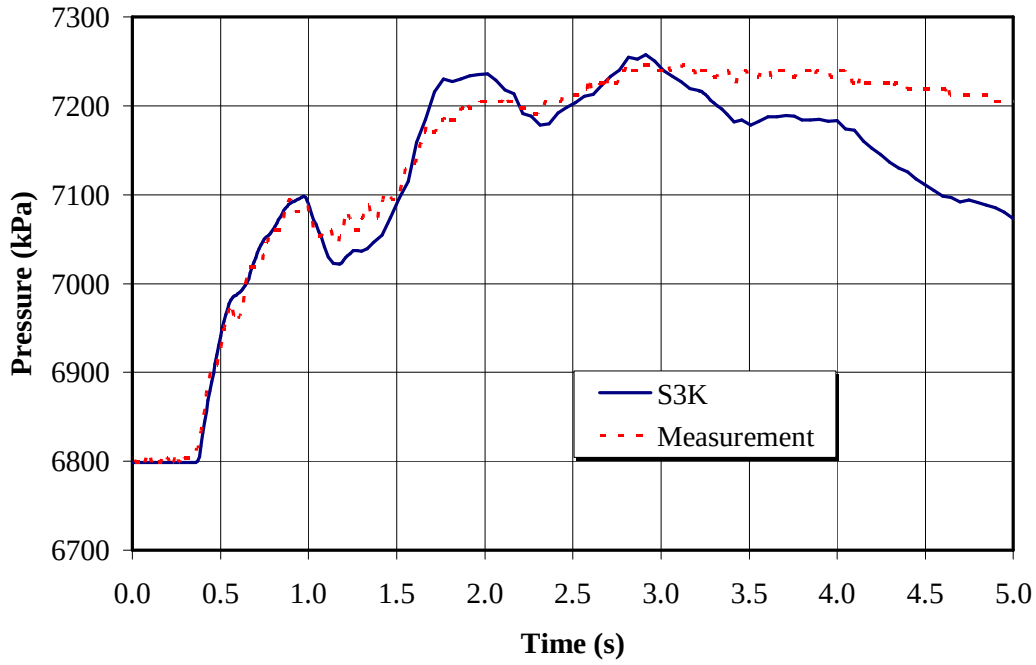

Figure 3. Behavior of the pressure in the steam dome during TT2.

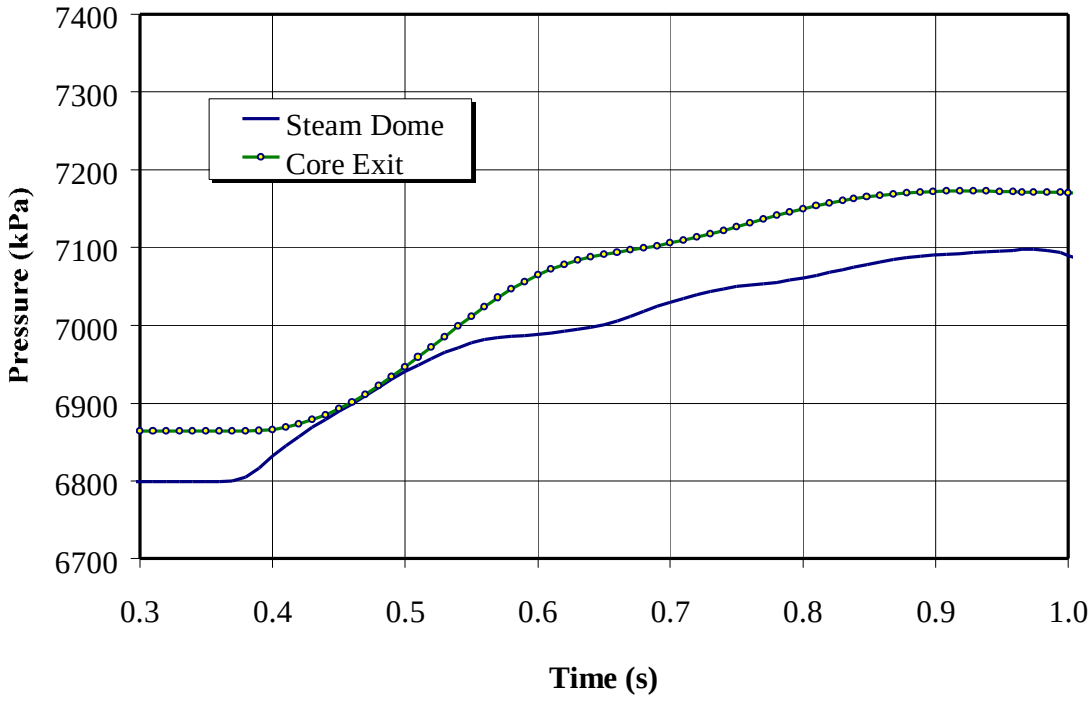

Figure 4. Calculated steam dome and core exit pressures.

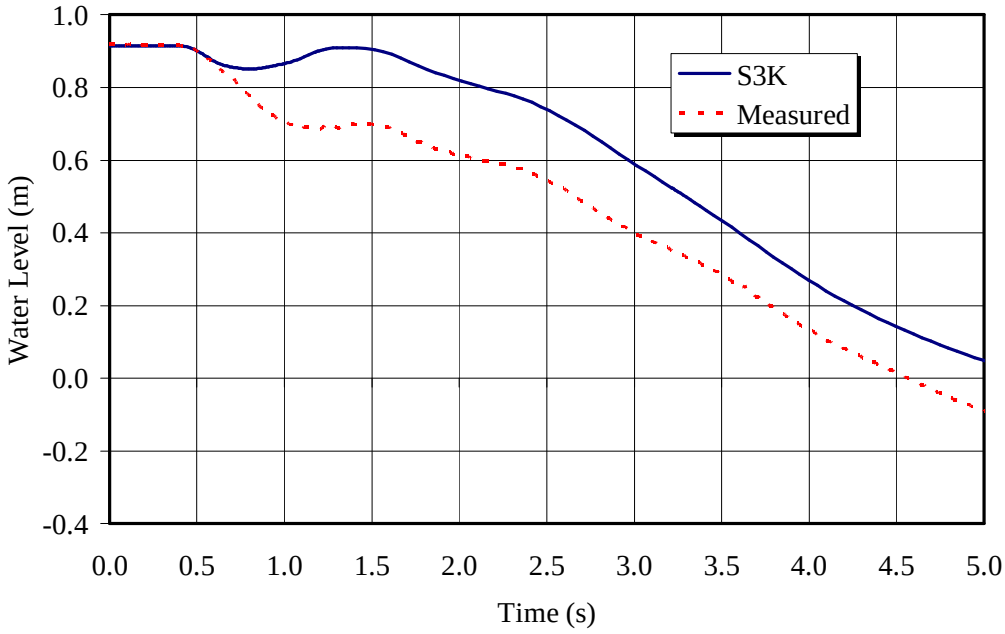

Figure 5. TT2 water level comparison.

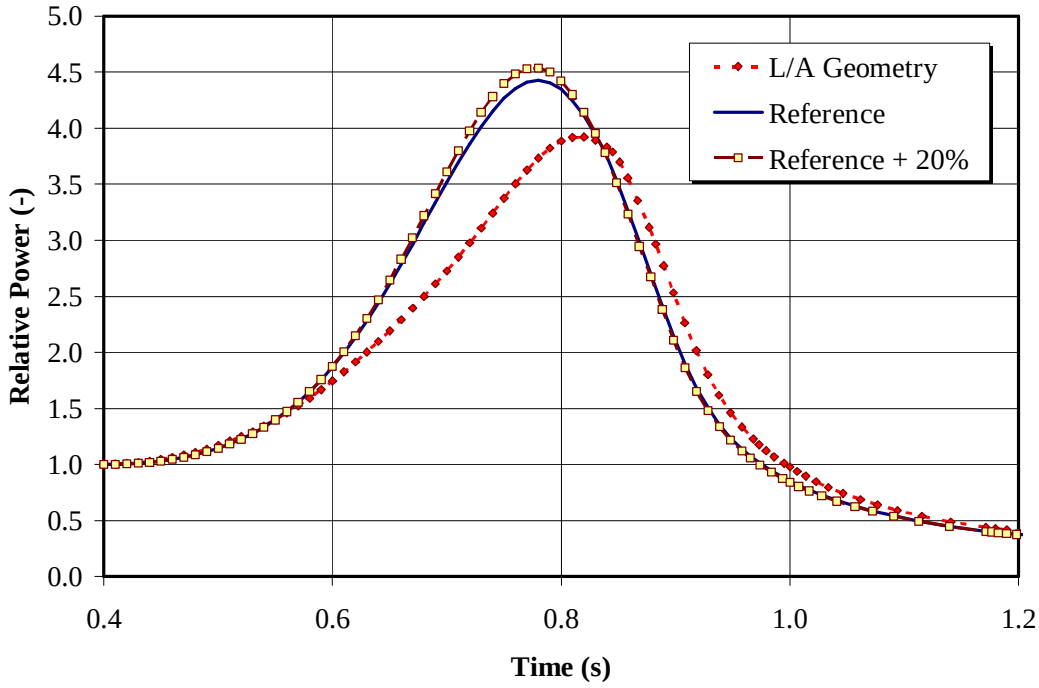

Figure 6. Power sensitivity to the steam separators inertia model.

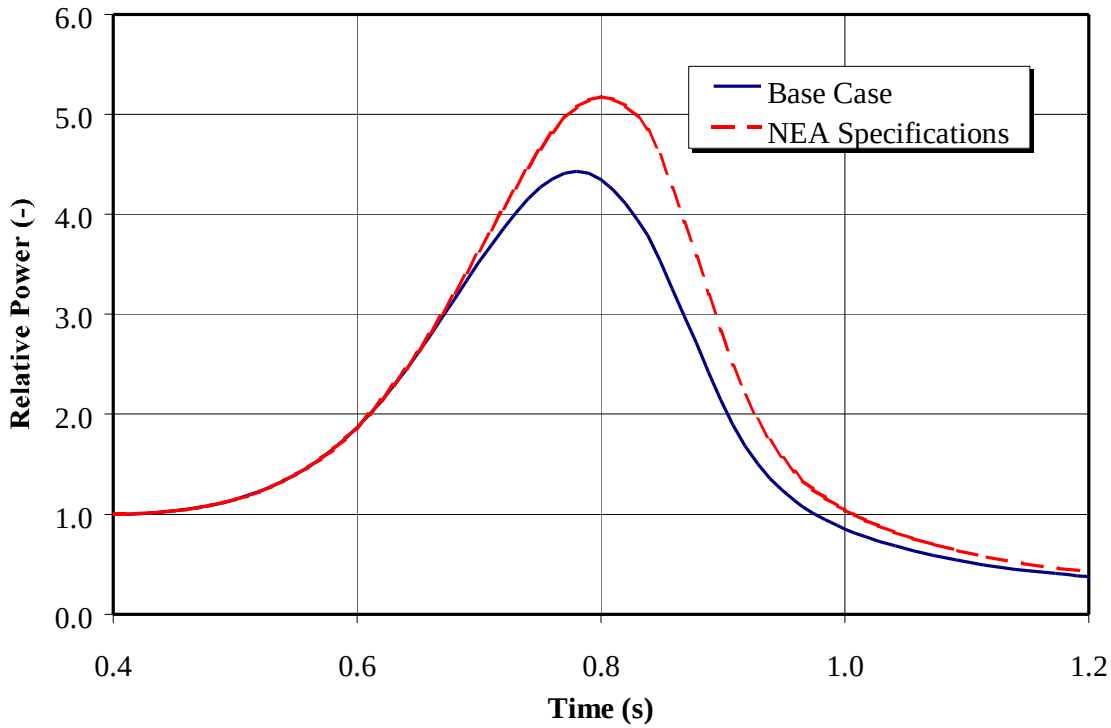

Figure 7. Effect of the gap conductance on the peak power.

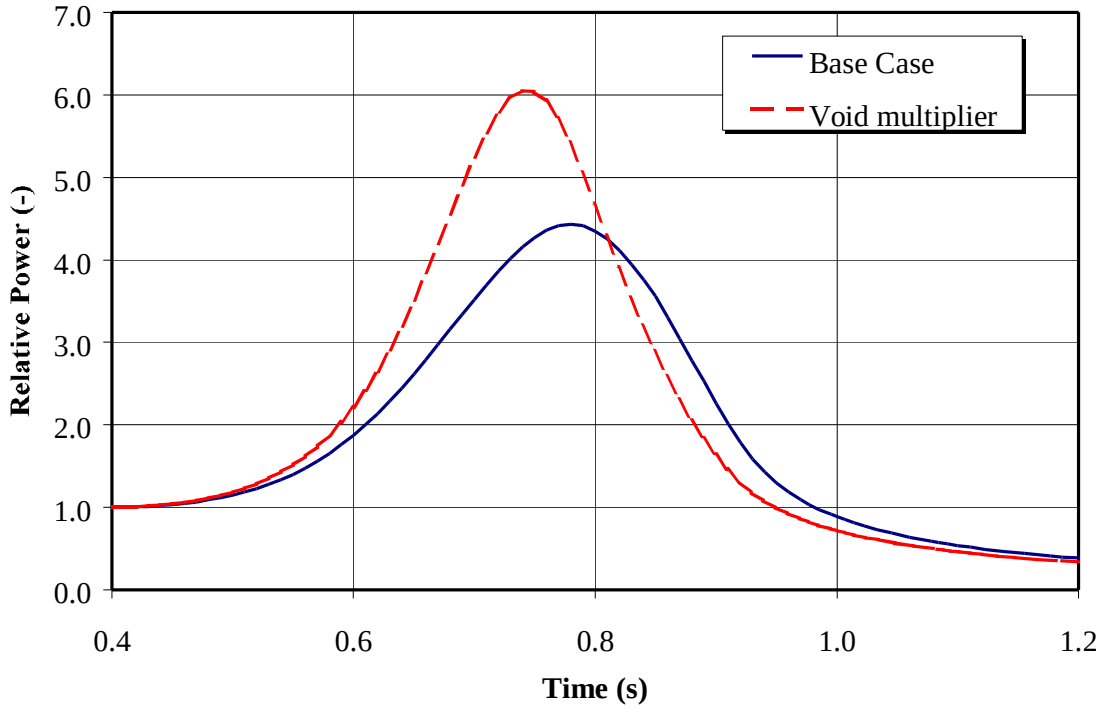

Figure 8. Effect of the void coefficient on power.

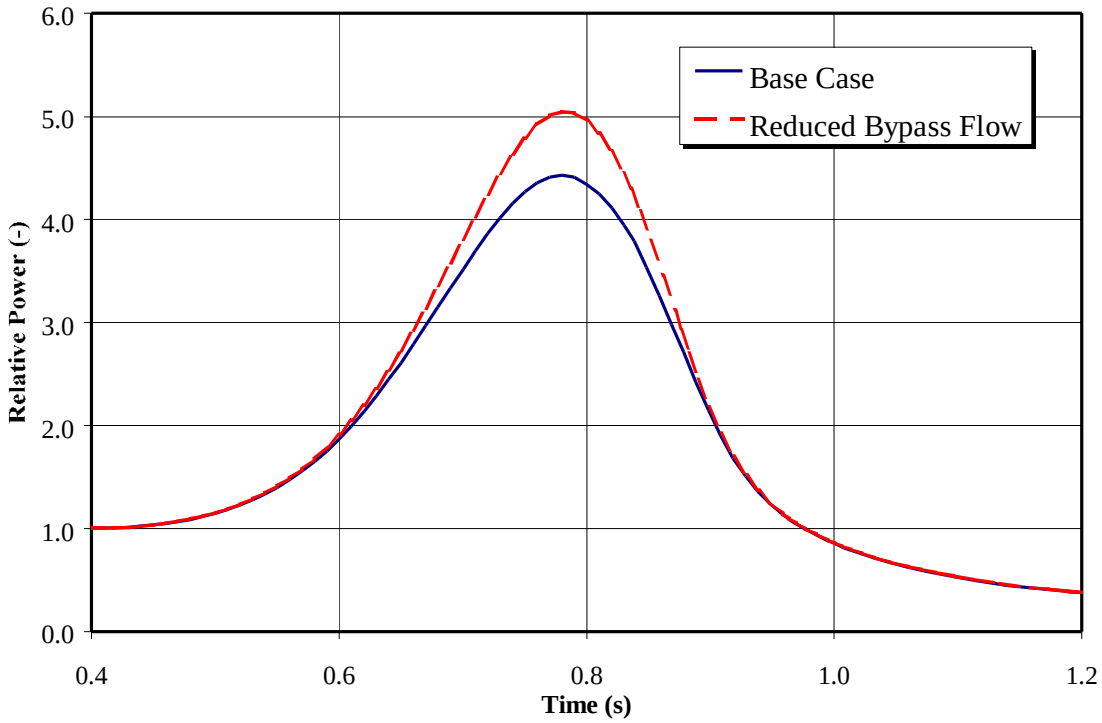

Figure 9. Sensitivity of the power to the bypass valve flow capacity.

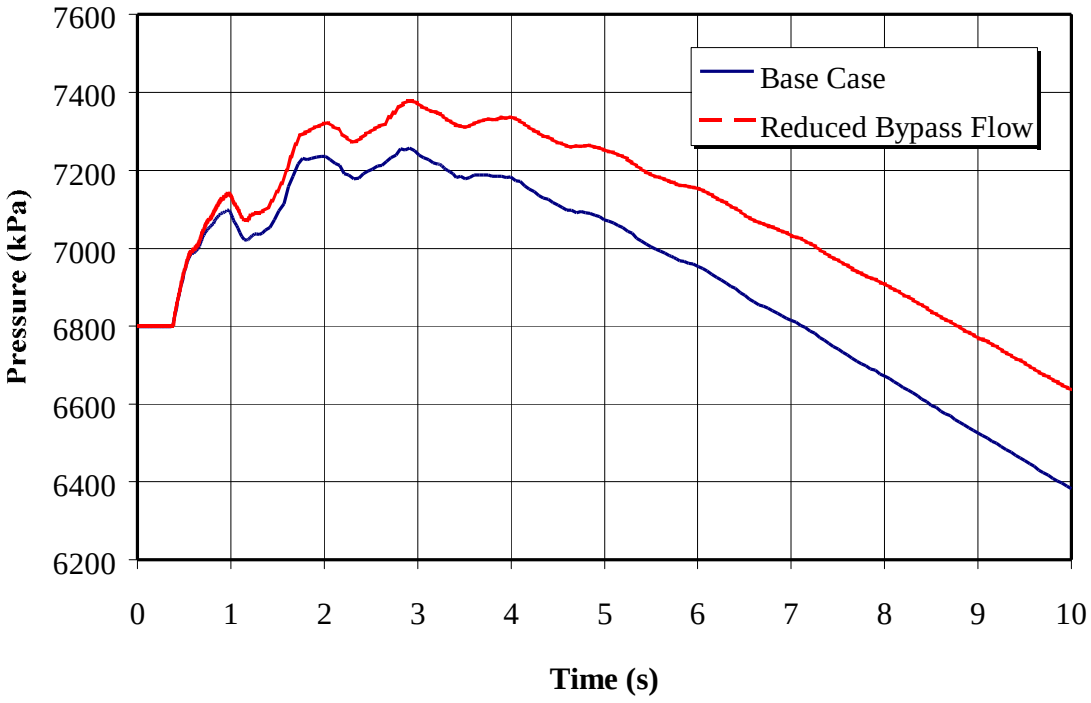

Figure 10. Sensitivity of the steam dome pressure to the bypass valve flow capacity.

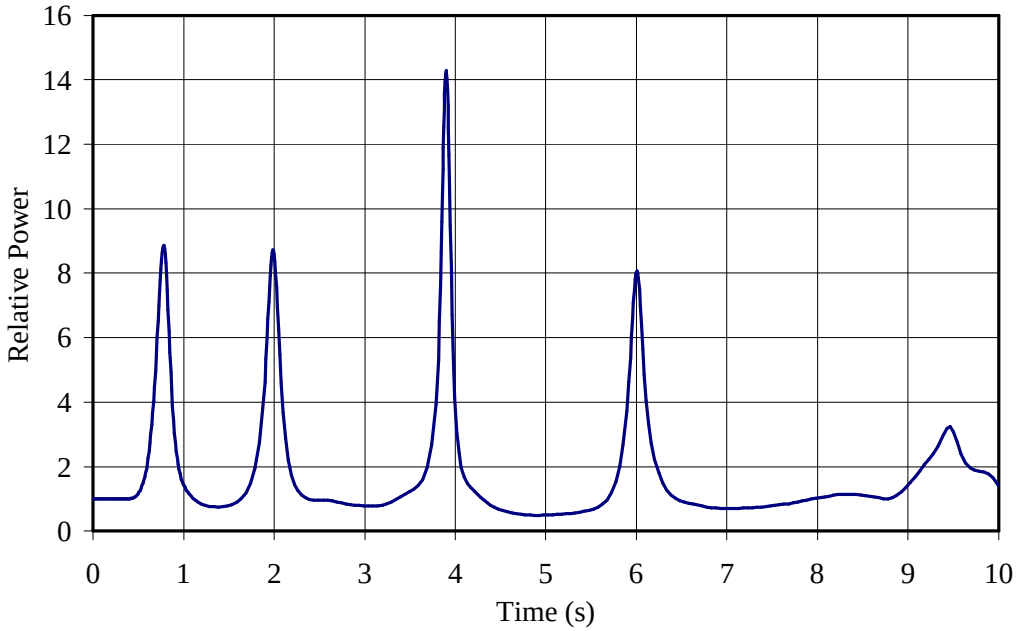

Figure 11. Relative power during a turbine trip with no scram and no bypass flow.

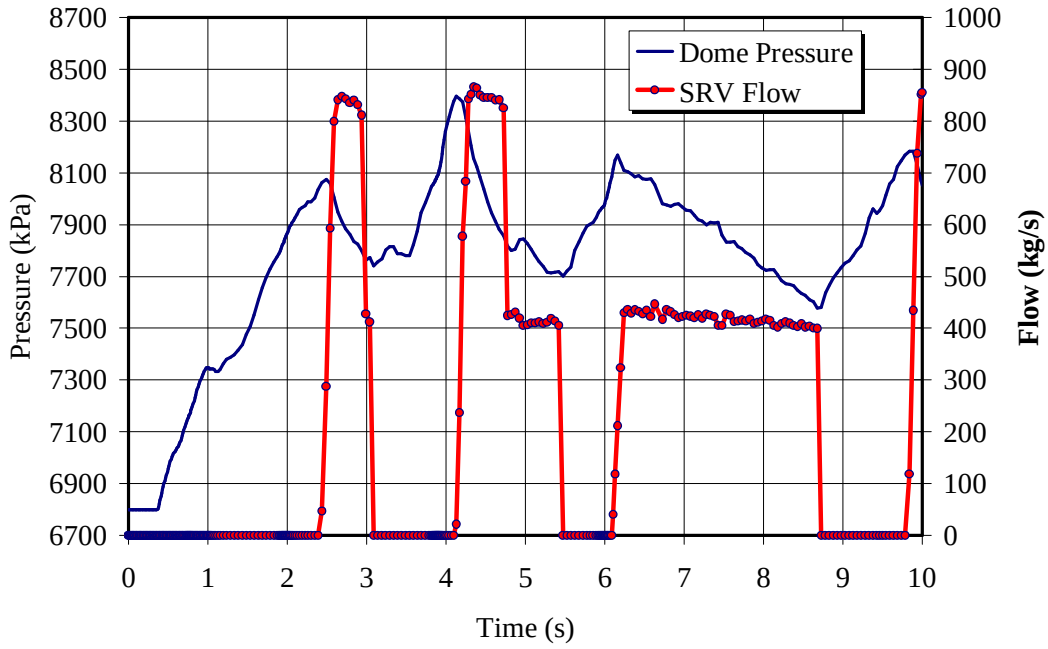

Figure 12. Dome pressure and SRV flow for TT with no scram and no bypass.